Universal behavior of scalar dissipation rate in confined porous media (Supplemental information)

Marco De Paoli,[1] Vlad Giurgiu,[1] Francesco Zonta,[1] and Alfredo Soldati[1,2]

[1] *Institute of Fluid Mechanics and Heat Transfer, TU Wien, 1060 Vienna, Austria*
[2] *Polytechnic Department, University of Udine, 33100 Udine, Italy*

Content of this file

Additional supporting information

1. Details on initial condition and diffusive regime

The initial concentration field is defined by:

$$C(x,z,t=0)=\frac{1}{2}\left[1+\mathrm{sgn}\left(\frac{z}{\mathrm{Ra}_0}-\frac{1}{2}\right)\right]+\varepsilon\ , \tag{S1}$$

with ε the initial perturbation, whereas the initial velocity field is set to zero ($u=w=0$). Note that the perturbation ε is applied only along the centerline, $z=\mathrm{Ra}_0/2$. As a consequence, the analytical solution of the solute balance equation, Eq. (2), is given by $C(\eta)=1/2\,[1+\mathrm{erf}\,(\eta)]$, where $\eta=(z-\mathrm{Ra}_0/2)/\sqrt{4t}$. From the definition of the mean scalar dissipation rate, and after some algebra, in the limit of small times and large Ra_0 we obtain:

$$\langle\chi\rangle=\frac{t^{-1/2}}{\sqrt{8\pi}}\,\mathrm{erf}\left(\frac{\mathrm{Ra}_0/2}{\sqrt{2t}}\right)\approx\frac{t^{-1/2}}{\sqrt{8\pi}}\ . \tag{S2}$$

We wish to remark that the evolution of the system depends on the amplitude of the initial perturbation ε. In particular, the role played by ε is crucial during the intermediate phase of the flow evolution, when fingers start to appear. This was also observed by De Paoli et al. [1], who noticed that the universal behavior of the mixing length, i.e. the tip-to-rear finger distance, became less robust during the transition from the diffusive to the convective regime.

To measure the sensitivity of the results to the initial perturbation, we performed simulations at all the Rayleigh-Darcy numbers considered using three different values of ε, namely $\mathcal{O}(\varepsilon)\in\{10^{-3},\,10^{-4},\,10^{-5}\}$, and we monitor the time behavior of the quantity $\mathcal{M}(t)$. Results, which are reported in Fig. S1 for $\mathrm{Ra}_0=7244$, show that the larger the initial perturbation, the sooner the profile departs from the analytical diffusive solution $t^{1/2}$. However, after a transition during which the fingers merge, the growth of $\mathcal{M}(t)$ is the same for all perturbations considered. Asymptotically, the value $\mathcal{M}_\infty=\mathrm{Ra}_0/8$ is attained. Note also that it is important to impose the same initial perturbation profile regardless of the value of Ra_0 by properly interpolating the concentration profile when changing the grid resolution.

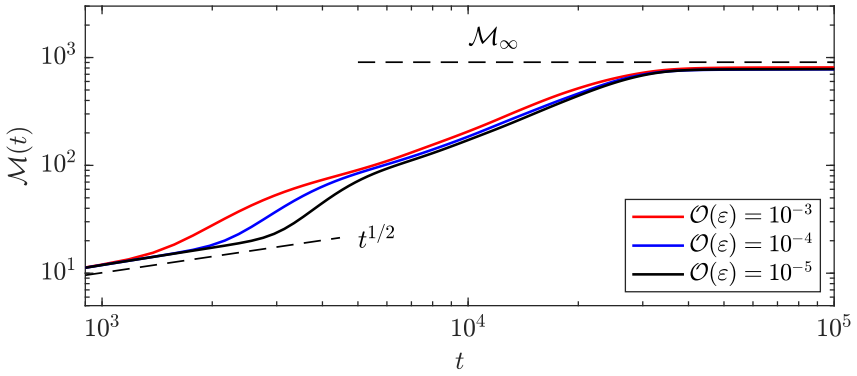

FIG. S1. The temporal evolution of $\mathcal{M}(t)$ for $\mathrm{Ra}_0=7244$ is here shown. We report the data corresponding to three different initial perturbations [$\mathcal{O}(\varepsilon)\in\{10^{-3},\,10^{-4},\,10^{-5}\}$]. Initially, the evolution is independent from the perturbation, since controlled by diffusion ($t^{1/2}$). For the intermediate regime, when the fingers merging occurs, the influence of the initial perturbation is effective. The saturation value $\mathcal{M}_\infty$, corresponding to $\mathrm{Ra}_0/8$, is attained asymptotically.

2. Physical meaning of the mean scalar dissipation rate

The mean scalar dissipation rate $\langle\chi\rangle$ is used to characterize porous media flows controlled by solute convection [2, 3]. To provide a further interpretation of $\langle\chi\rangle$ as an indicator of mixing/convection, we extend the analysis of $\langle\chi\rangle$ and its dynamics to two other flow configurations that are frequently taken as important archetypes for geophysical flows: The Rayleigh-Bénard and the one-sided configuration.

We consider a two-dimensional and rectangular porous layer fully saturated by an incompressible fluid. The system is controlled by Eqs. (1)-(2). We assume that the domain is periodic in horizontal direction and is confined by two horizontal walls, along which either the concentration is fixed or the solute flux through the wall is set to zero. After some algebraic manipulations, the solute transport equation (2) integrated over the domain gives [2]:

$$\frac{\partial\langle C^2\rangle}{\partial t} = 2(C_{top}F_{top} + C_{bot}F_{bot} - \langle\chi\rangle), \tag{S3}$$

where C_{top} (C_{bot}) is the concentration at the top (bottom) boundary, $F_{top} = \overline{\partial C/\partial z}|_{z=\mathrm{Ra}_0}$ and $F_{bot} = \overline{\partial C/\partial z}|_{z=0}$ are the fluxes across the top and bottom boundaries, with $\bar{\cdot} = L^{-1}\int_0^L \cdot\, \mathrm{d}x$ indicating the average over the horizontal direction. Eq. (S3) can be also used in this form as an indicator to check the accuracy of the results obtained [4].

All the systems considered in this section are characterized by the same value of the governing parameter $\mathrm{Ra}_0 = 7244$.

a) Rayleigh-Bénard system [Fig. S2(a-i)-(a-ii)]: the concentration is fixed at the upper ($C_{top} = 1$) and lower ($C_{bot} = 0$) boundaries. After a transition phase that depends on the initial concentration field, the flow enters a statistically steady-state regime [3, 5, 6], which is independent of the initial condition. We indicate with $\bar{\bar{\cdot}} = 1/T\int_{t-T/2}^{t+T/2} \cdot\, \mathrm{d}t$ the time-average operator and we compute the time-average form of Eq. (S3), which is

$$\bar{\bar{F}} = \overline{\overline{\langle\chi\rangle}}\ , \tag{S4}$$

since $\overline{\overline{\partial_t\langle C^2\rangle/2}} = 0$ and $F = F_{top}$ [3]. However, the term $\partial_t\langle C^2\rangle/2$ may be instantaneously either positive or negative, as shown in Fig. S2(a-i). The expected (theoretical) behavior of the steady state value $\bar{\bar{F}}$ can be evaluated with the correlation proposed by Hewitt et al. [7] and adapted to the present dimensionless set of variables. In particular, we have $\bar{\bar{F}} = (0.00688\,\mathrm{Ra}_0 + 2.75)/\,\mathrm{Ra}_0$ [dashed line in Fig. S2(a-i)], which is independent from the Rayleigh-Darcy number in the limit of high Ra_0.

b) One-sided system [Fig. S2(b-i)-(b-ii)]: the domain is initially filled with pure fluid [$C(x, z, t = 0) = 0$] and the concentration is fixed at the top boundary ($C_{top} = 1$). The systems is closed with respect to solute fluxes across the lower boundary ($F_{bot} = 0$). With these constraints, Eq. (S3) gives

$$\frac{\partial\langle C^2\rangle}{\partial t} = 2\left(F - \langle\chi\rangle\right)\ , \tag{S5}$$

where $F = F_{top}$. The evolution of the one-sided configuration is time-dependent (see De Paoli et al. [8] for a description of the whole dissolution process). However, after

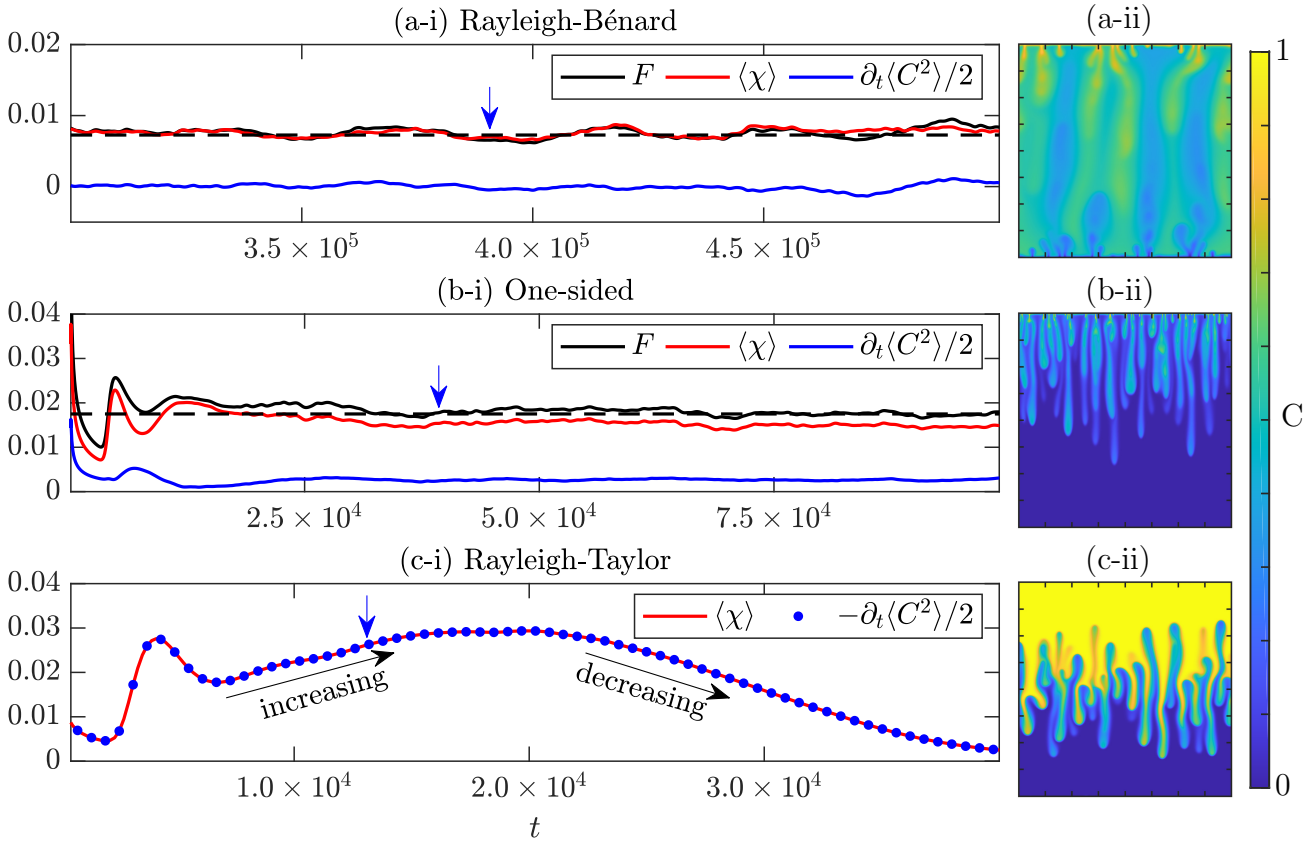

FIG. S2. Three different flow configurations are here considered: (a) Rayleigh-Bénard, (b) One-sided and (c) Rayleigh-Taylor. In all the three cases, $\mathrm{Ra}_0 = 7244$. Left panels: evolution of the parameters $\langle\chi\rangle$, F and $\partial_t\langle C^2\rangle/2$. Right panels: exemplar concentration fields taken at the times indicated by the blue arrows in panels (a-i), (b-i) and (c-i), during the convection-dominated regime. The expected value of F is also reported (dashed lines) in panels (a-i) and (b-i).

an initial diffusive regime, the dissolution rate F is nearly constant [7–11] and equal to approximately 0.017 [dashed line in Fig. S2(b-i)]. A similar behavior of $\langle\chi\rangle$ is observed in the instance of a Rayleigh-Taylor system characterized by a non-monotonic density-concentration profile [2, 12].

c) Rayleigh-Taylor system [Fig. S2(c-i)-(c-ii)]: the boundaries are impermeable with respect to solute fluxes ($F_{top} = F_{bot} = 0$). The concentration field is initialized with an unstable density profile in which $C(x, z > \mathrm{Ra}_0/2, t = 0) = 1$ [$C(x, z < \mathrm{Ra}_0/2, t = 0) = 0$] in the upper [lower] half of the domain. Therefore, Eq. (S3) gives

$$\frac{\partial\langle C^2\rangle}{\partial t} = -2\langle\chi\rangle. \tag{S6}$$

After an initial phase in which diffusion dominates, fingers form and merge [1]. Then, a convection-dominated regime occurs, and $\langle\chi\rangle$ is observed to grow. After impingement of the fingers on the boundaries, the mean scalar dissipation rate decreases due to

the reduction of the local concentration differences induced by the saturation of the domain.

We observe that a regime in which the flow is dominated by convection exists in these three configurations. However, some differences occur: while in cases a) and b) $\langle\chi\rangle$ is statistically constant and slightly decreasing respectively, in case c) a growth of $\langle\chi\rangle$ is observed. This increase is only arrested when the fingers reach the boundaries of the domain.

3. Caption for "Movie S1"

Time-dependent evolution of a system characterized by Rayleigh-Darcy number $\mathrm{Ra}_0 = 12023$ and amplitude of the initial perturbation $\mathcal{O}(\varepsilon) = 10^{-5}$. (a) Concentration distribution with explicit indication of the finger extension (mixing length, red dashed lines). (b) Horizontally-averaged concentration profile. (c) Time dependent evolution of $\mathcal{M}(t)$.

4. Caption for "Movie S2"

Time-dependent evolution of a system characterized by Rayleigh-Darcy number $\mathrm{Ra}_0 = 12023$ and amplitude of the initial perturbation $\mathcal{O}(\varepsilon) = 10^{-5}$. (a) Scalar dissipation rate distribution. (b) Horizontally-averaged scalar dissipation rate profile. (c) Time-dependent evolution of $\langle\chi(t)\rangle$.

5. Caption for "Movie S3"

Time-dependent evolution of a system characterized by Rayleigh-Darcy number $\mathrm{Ra}_0 = 12023$ and amplitude of the initial perturbation $\mathcal{O}(\varepsilon) = 10^{-5}$. (a) Scalar dissipation rate distribution. (b) Power spectrum computed along the centerline. (c) Time-dependent evolution of mean wavenumber.

---

[1] M. De Paoli, F. Zonta, and A. Soldati. Rayleigh-Taylor convective dissolution in confined porous media. *Phys. Rev. Fluids*, 4:023502, Feb 2019.

[2] J. J. Hidalgo, J. Fe, L. Cueto-Felgueroso, and R. Juanes. Scaling of convective mixing in porous media. *Phys. Rev. Lett.*, 109(26):264503, 2012.

[3] J. Otero, L. A. Dontcheva, H. Johnston, R. A. Worthing, A. Kurganov, G. Petrova, and C. R. Doering. High-Rayleigh number convection in a fluid-saturated porous layer. *J. Fluid Mech.*, 500:263–281, 2004.

[4] T. Le Borgne, M. Dentz, D. Bolster, J. Carrera, J. R. De Dreuzy, and P. Davy. Non-fickian mixing: Temporal evolution of the scalar dissipation rate in heterogeneous porous media. *Adv. Water Resour.*, 33(12):1468–1475, 2010.

[5] D. R. Hewitt, J. A. Neufeld, and J. R. Lister. Ultimate regime of high Rayleigh number convection in a porous medium. *Phys. Rev. Lett.*, 108(22):224503, 2012.

[6] M. De Paoli, F. Zonta, and A. Soldati. Influence of anisotropic permeability on convection in porous media: implications for geological CO2 sequestration. *Phys. Fluids*, 28(5):056601, 2016.

[7] D. R. Hewitt, J. A. Neufeld, and J. R. Lister. Convective shutdown in a porous medium at high Rayleigh number. *J. Fluid Mech.*, 719:551–586, 2013.

[8] M. De Paoli, F. Zonta, and A. Soldati. Dissolution in anisotropic porous media: Modelling convection regimes from onset to shutdown. *Phys. Fluids*, 29(2):026601, 2017.

[9] G. S. H. Pau, J. B. Bell, K. Pruess, A. S. Almgren, M. J. Lijewski, and K. Zhang. High-resolution simulation and characterization of density-driven flow in CO2 storage in saline aquifers. *Adv. Water Resour.*, 33(4):443–455, 2010.

[10] A. C. Slim. Solutal-convection regimes in a two-dimensional porous medium. *J. Fluid Mech.*, 741:461–491, 2014.

[11] B. Wen, D. Akhbari, L. Zhang, and M. A. Hesse. Convective carbon dioxide dissolution in a closed porous medium at low pressure. *J. Fluid Mech.*, 854:56–87, 2018.

[12] J. J. Hidalgo, M. Dentz, Y. Cabeza, and J. Carrera. Dissolution patterns and mixing dynamics in unstable reactive flow. *Geophys. Res. Lett.*, 42(15):6357–6364, 2015.